ELSEVIER

Journal of Chromatography A, 712 (1995) 253–268

JOURNAL OF CHROMATOGRAPHY A

Mass spectral analyses of microcystins from toxic cyanobacteria using on-line chromatographic and electrophoretic separations ☆

K.P. Bateman[a,b], P. Thibault[b,*], D.J. Douglas[b], R.L. White[a]

[a]*Chemistry Department, Dalhousie University, Halifax, NS, B3H 4J3 Canada*

[b]*Institute for Marine Biosciences, National Research Council of Canada, 1411 Oxford Street, Halifax, NS, B3H 3Z1 Canada*

Abstract

The application of capillary electrophoresis and of reversed-phase liquid chromatography coupled to electrospray mass spectrometry is presented for the analysis of microcystins isolated from toxic strains of *Microcystis aeruginosa*. The separation performance of these two techniques is compared in terms of both sensitivity and of resolution of closely related microcystins. Quantitation of microcystin-LR present at low μg/ml concentrations in cell extracts is demonstrated using both techniques. A marked advantage of capillary electrophoresis over liquid chromatography was its ability to resolve different desmethyl microcystin-LR analogues. Identification of these positional isomers was facilitated using capillary electrophoresis combined with tandem mass spectrometry (MS–MS). Rationalization of fragment ions observed in MS–MS spectra of microcystins was made possible through comparison with ^{15}N labelled microcystins obtained from stable isotope feeding experiments. The potential of tandem mass spectrometry in providing selective detection of microcystins in cell extracts, and in structural characterization of novel microcystins, was also investigated.

1. Introduction

Microcystins are unusual cyclic peptides produced by toxic strains of the cyanobacteria *Microcystis*, *Anabaena*, *Nostoc*, and *Oscillatoria* [1,2]. These peptides are potent hepatotoxins [3–5] causing substantial disruption of the liver architecture, rearrangement of cellular organelles, and reorganization of microfilaments [6–10]. In contrast to other forms of algal poisoning, this type of intoxication is characterized by the appearance of a dark mottled liver, swollen with blood to twice its normal weight [2]. Acute dosage in mice can lead to rapid death of the animal between 30 min and 3 h, and the LD_{50} in a mouse (intraperitoneal injection) is 40–800 μg/kg [11–14]. More recently, microcystins have been shown to be specific inhibitors of protein phosphatases 1 and 2A [15–17] and to also act as tumor promoters [18,19]. Changes in the balance of the phosphorylation and dephosphorylation reactions of proteins is thought to be a key element in the modifications of the microfilament structures and hepatocyte morphology [4–10]. In view of their toxicity and the world-wide occurrence of toxic cyanobacterial blooms, microcystins thus present a serious global health problem in water supplies, both for livestock and humans [20–22].

The microcystins belong to a family of cyclic heptapeptides with the general structure cyclo-D-

* Corresponding author.

☆ NRCC: 38100.

SSDI 0021-9673(95)00438-6

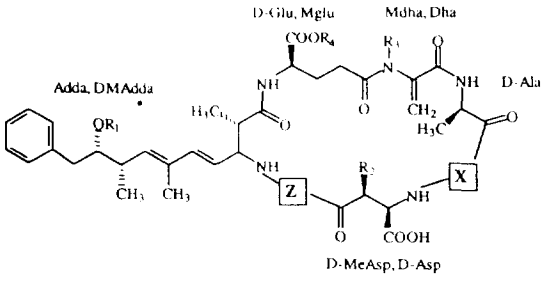

Microcystin	X	Z	R_1	R_2	R_3	R_4	MW (Da)
D-Asp-LR	Leu	Arg	CH_3	H	CH_3	H	980.5
Dha-LR	Leu	Arg	CH_3	CH_3	H	H	980.5
DMAdda-LR	Leu	Arg	H	CH_3	CH_3	H	980.5
AR	Leu	Ala	CH_3	CH_3	CH_3	H	952.4
VF	Val	Phe	CH_3	CH_3	CH_3	H	971.5
LF	Leu	Phe	CH_3	CH_3	CH_3	H	985.5
LR	Leu	Arg	CH_3	CH_3	CH_3	H	994.5
LY	Leu	Tyr	CH_3	CH_3	CH_3	H	1001.5
Mglu-LR	Leu	Arg	CH_3	CH_3	CH_3	CH_3	1008.5
LW	Leu	Trp	CH_3	CH_3	CH_3	H	1024.5

Fig. 1. Structure of microcystin-LR and other substituted hepatotoxins. Major sites of amino acid substitution are indicated by the letters **X** and **Z** in the cyclic structure

Ala-L-(**X**)-*erythro*-β-methyl-D-isoaspartic acid-L-(**Z**)-Adda-D-isoglutamic acid-N-methyldehydroalanine (Fig. 1), where **X** and **Z** represent variable L-amino acids, and Adda is 3-amino-9-methoxy-2,6,8-trimethyl-10-phenyldeca-4,6-dienoic acid [23–26]. To date 47 different analogues have been identified [21]. The most common microcystin has leucine and arginine in the **X** and **Z** position, respectively, and is designated microcystin-LR (Fig. 1) [27].

The need for reliable, rapid, and sensitive methods for the identification of microcystins in the environment has been prompted by the increased awareness of toxic cyanobacterial blooms and their associated human-health problems. Cyanobacterial toxins can be detected using the mouse bioassay [1] and protein phosphatase (PPase) assay [28,29]. Bioassays based on cultured bacterial cells have also been developed, but were found to be non-specific [30,31]. An enzyme-linked immunosorbent assay (ELISA) [32] has been developed, but the antibodies show little cross-reactivity with some microcystins. Alternative screening methods are often desired in view of the non-specific nature of the assays, the potential for false-positives [28], and also because of social pressure to ban animal testing.

Existing instrumental methods used for the detection and quantification of microcystins depend mainly on reversed-phase liquid chromatography (LC) with ultraviolet (UV) detection at 238 nm [33–35]. The use of a diode-array detector allows detection of total microcystins based on spectral match, even if standards are not available [36,37]. Recently, an LC-linked PPase screening method was developed for the identification of okadaic acid [38]. Suspected fractions from marine and freshwater samples were subsequently analyzed for diarrhetic shellfish poisoning toxins and microcystins using capillary electrophoresis [39,40].

Mass spectrometry using the fast atom bombardment (FAB) ionization technique has also been applied to the identification and quantification of microcystins. Accurate mass measurements and tandem mass spectrometry (MS–MS) were used to obtain empirical formulae and structural information [12,41–47]. Applications of LC combined with MS, using ionization techniques such as frit-FAB [48] and nebulizer-assisted electrospray (ionspray) [37,49], were also described recently for the identification of microcystins in cyanobacterial extracts. Edwards et al. [37] demonstrated the use of tandem mass spectrometry combined with liquid chromatography (LC–MS–MS) for the analysis of purified microcystins. They described the possibility of incorporating the precursor-ion scans of m/z 135, a fragment ion formed from the Adda side-chain, into an LC–MS–MS screening method. Such a procedure would be of particular interest in view of the fact that the toxicity of microcystins appears to be associated with the presence of the Adda residue [15,50].

Work in our laboratory on interfacing capillary electrophoresis (CE) with ionspray ionization MS has shown the technique to be applicable to the analysis of a variety of biological compounds, including marine toxins [51,52] and peptides [53]. CE is complementary to LC, and offers the advantages of high separation efficiencies and

reduced sample sizes. The present report describes the use of LC and CE combined with electrospray mass spectrometry (ESMS) for the identification and quantitation of microcystins in extracts of different strains of *Microcystis aeruginosa*. Tandem mass spectrometry combined with either LC or CE separations was used to characterize the structures of previously unknown microcystins.

2. Experimental

2.1. Chemicals

Microcystin-LR was obtained from ICN Biomedicals (Aurora, OH, USA). HPLC-grade acetonitrile and methanol were obtained from Caledon Laboratories (Georgetown, Canada). Distilled and deionized (18 MΩ) water (Milli-Q water systems, Millipore, Bedford, MA, USA) was used in the preparation of samples and buffer solutions.

2.2. Cell cultures

Microcystis aeruginosa strains PCC 7820 (Pasteur Culture Collection, Paris, France) and UTEX LB 2385 (The Culture Collection of Algae, University of Texas at Austin, TX, USA) were grown in BG-11 [43] culture medium under fluorescent illumination (Cool-White) on a 12 h:12 h light:dark cycle at 20°C. Stable isotope feeding experiments used ^{15}N-labelled $NaNO_3$ at a concentration of 1 g/l (97.5 at%, MSD isotopes, Montreal, Canada) as a substitute for the unlabelled nitrate in BG-11.

2.3. Extraction of microcystins

Cell material was sonicated for 10 min in 25% methanol (0.5 g/50 ml wet weight) and the sonicated slurry was stirred for 20 min to permit optimum extraction. After centrifugation at 3000 *g* for 10 min the supernatant was collected and the pellet re-extracted. The supernatant was concentrated using a rotary evaporator to approximately 10 ml. The concentrated supernatant was applied to a pre-conditioned C_{18} Sep-Pak column (Waters, Milford, MA, USA). The cartridge was washed with water (2 × 10 ml) and microcystins were eluted with 100% methanol (2 × 10 ml). The methanol was removed using a Speedvac concentrator, and the residue stored at −10°C until required. Samples were dissolved in 40% aqueous methanol for analysis.

2.4. High-performance liquid chromatography with UV detection

All HPLC–UV experiments were performed using a Hewlett-Packard (Palo Alto, CA, USA) HP1090 Series II liquid chromatograph equipped with a ternary DR5 solvent delivery system, an HP1040A diode-array detector, and an HP7994A data system. Microcystins were separated on a 2.1 × 250 mm Vydac 218TP52 column (Vydac Separation group, Hisperia, CA, USA) using a linear gradient elution of 10–60% acetonitrile (0.1% trifluoroacetic acid) in 20 min, followed by a 5 min hold at 60% acetonitrile. The UV absorbance was monitored at both 214 and 238 nm, but full UV spectra were acquired once a chromatographic peak was detected. Sample injection volumes were typically 10 μl.

2.5. Capillary electrophoresis with UV detection

Analyses of microcystins by CE–UV were achieved using a P/ACE System 2100 (Beckman Instruments, Fullerton, CA, USA). The instrument was equipped with a variable-wavelength UV detector using through-column optics. The system was interfaced directly to an MS-DOS computer (80386 processor) using a Beckman System Gold dedicated software package. Separations were performed using bare fused-silica capillaries (Polymicro Technologies, Phoenix, AZ, USA) previously coated with an aqueous solution of 5% (w/v) hexadimethrine bromide (Polybrene, Aldrich Chemicals, Milwaukee, WI, USA), and 2% (w/v) ethylene glycol (Aldrich). Separations using dynamically coated capillaries were conducted using 50-μm I.D. × 107-cm

length (100 cm to detector) columns with 1 *M* formic acid buffer. The CE–UV analyses were performed using polarity reversal by applying a voltage of −30 kV at the injector end of the capillary.

2.6. Mass spectrometry

Mass spectra were obtained using a Perkin–Elmer SCIEX API/III$^+$ triple quadrupole mass spectrometer (Thornhill, Canada) equipped with a fully articulated, pneumatically assisted nebulization probe and an atmospheric pressure ionization source operated in electrospray (ionspray) mode. LC–ESMS analyses used the same chromatographic system as that described above except that a flow splitter was mounted after the HPLC column, thus allowing a flow-rate of only 15 μl/min to the mass spectrometer. All CE–ESMS experiments were performed using an ATI Unicam Crystal CE System (Madison, WI, USA). A separate power supply (Glassman EH Series, Glassman, Whitehouse Station, NJ, USA) was used to provide an electrospray voltage of 5 kV. The CE–ESMS interface is based on a coaxial column arrangement [54] which was subsequently modified in our laboratory [51]. A more detailed description of the interface configuration has been presented elsewhere [52].

Mass spectral acquisition was performed using a dwell time of 4 ms per step of 1 dalton in full mass scan mode or 100 ms per channel in selected ion monitoring (SIM) experiments. Product ion spectra obtained from combined CE–MS–MS and LC–MS–MS analyses were obtained using collisional activation with argon target gas in the second (RF-only) quadrupole. Collision energies were typically 50 eV in the laboratory frame of reference, and the collision gas thickness was $3.5 \cdot 10^{15}$ atoms/cm^2. Tandem mass spectra were acquired using dwell times of 3 ms per step of 0.2 daltons in full-scan mode or 80 ms per channel in multiple reaction monitoring (MRM) experiments. A MacIntosh Quadra 950 computer was used for instrument control, data acquisition, and data processing.

3. Results and discussion

3.1. LC–UV and LC–ESMS analyses of cyanobacterial extracts

The LC–UV separation of microcystins extracted from *Microcystis aeruginosa* PCC 7820 is shown in Fig. 2. A non-specific response profile was generated by monitoring UV absorbance at 214 nm (Fig. 2a), whereas more selective detection of potential microcystins was achieved using a wavelength of 238 nm, corresponding to the chromophore of the unconjucated diene of the Adda residue (Fig. 2b). Microcystin-LR is observed in Fig. 2b as an intense peak eluting at 17.4 min, and other potential microcystins were

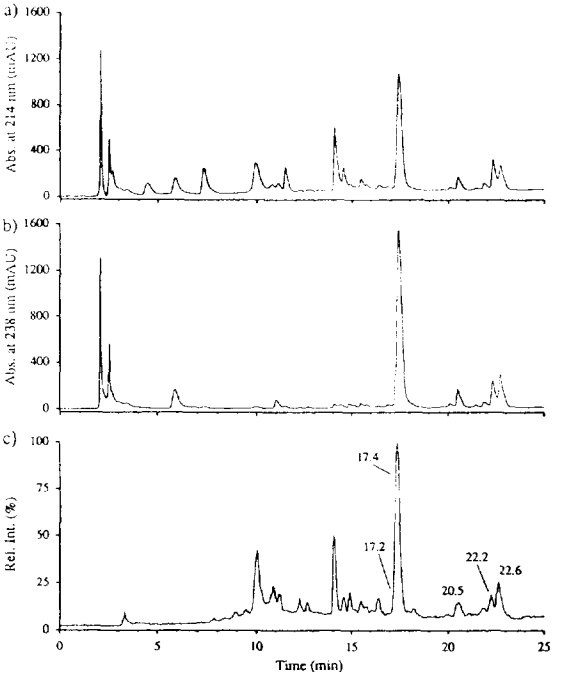

Fig. 2. Analysis of an extract from *M. aeruginosa* PCC 7820 using LC–UV at 214 nm (a), 238 nm (b), and LC–ESMS under full mass scan acquisition (*m/z* 400–1100) (c). Conditions: injection of 10 μl of a methanolic extract on a Vydac 218TP52 HPLC column, 0.2 ml/min flow-rate, linear gradient of 10–60% aqueous acetonitrile (0.1% trifluoroacetic acid), LC–ESMS conditions used a post-column splitter allowing only 15 μl/min flow-rate to the mass spectrometer.

observed between 20 and 23 min. However, no structural assignments of these compounds could be made, due to the lack of available standards. In addition to the typical absorption at 238 nm, the UV spectra of several of these suspected microcystins showed characteristic features suggesting the presence of aromatic amino acids. For example, the peak eluting at 22.6 min in Fig. 2b showed a strong absorption band at 280 nm characteristic of a tryptophan residue.

The total ion chromatogram (TIC), obtained by LC–ESMS analysis of the same algal extract, is shown in Fig. 2c. The TIC corresponding to the full mass scan acquisition (m/z 400–1100) gave a profile qualitatively similar to that of the LC–UV at 214 nm (Fig. 2a). Some of the early eluting peaks observed between 3 and 8 min in Fig. 2a, were not detected in the LC–ESMS analysis, and were possibly compounds with molecular masses outside the selected scan range. Examples of extracted mass spectra taken from the LC–ESMS analysis shown in Fig. 2c are presented in Fig. 3. The mass spectrum of microcystin-LR (Fig. 3b) is dominated by ions corresponding to singly and doubly protonated molecules, $[M+H]^+$ and $[M+2H]^{2+}$, at m/z 996 and 498, respectively.

Tentative structural assignments of other microcystin structures could be deduced from molecular mass measurements taken from the extracted mass spectra. For example, Fig. 3a shows the mass spectrum of a potential microcystin corresponding to a desmethyl analogue of microcystin-LR (m/z 982). This compound eluted at 17.2 min in Fig. 2c, and appeared as a shoulder on the microcystin-LR peak. Three different desmethyl microcystin-LR isomers have been reported in the literature, including desmethyl-Adda-LR [12], dehydroalanine-LR [12,36,47] and D-aspartic acid-LR [36,41,46]. Unfortunately, it was not possible to further determine the identity of this desmethylated analogue, nor was it possible to establish whether the sample contained more than one isomer. The peak detected at 20.5 min (Fig. 3c) showed an intense $[M+H]^+$ ion at m/z 1003, and was consistent with microcystin-LY [55].

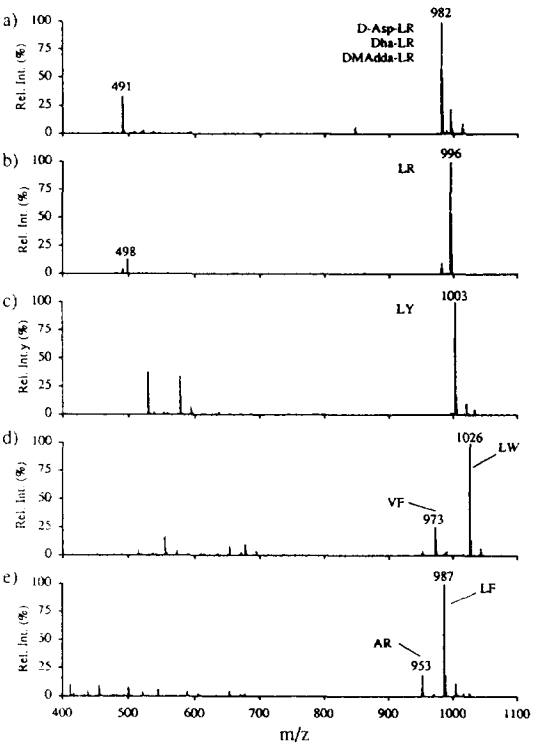

Fig. 3. Extracted mass spectra for peaks eluting at 17.2 (a), 17.4 (b), 20.5 (c), 22.2 (d), and 22.6 min (e) in Fig. 2c.

Two co-eluting microcystins, for which abundant $[M+H]^+$ ions were observed at m/z 953 and 987 (Fig. 3e), were tentatively assigned as microcystin-AR [12] and microcystin-LF [56], respectively. Finally, the extracted mass spectrum for the peak detected at 22.2 min is presented in Fig. 3d, and shows two $[M+H]^+$ ions at m/z 973 and 1026. As mentioned above, the UV spectrum for this peak showed a typical absorption band at 280 nm characteristic of a tryptophan residue. The higher molecular mass component at m/z 1026 was tentatively assigned as microcystin-LW. To the best of our knowledge, no report has documented thus far the production of this microcystin from cultures of *M. aeruginosa* or any other toxic cyanobacteria. The molecular mass of the smaller component observed at m/z 973 in Fig. 3d could not be matched with that of any of the known microcystins [21], and further

experiments using tandem mass spectrometry (see following section) were required to provide insights on the structure of this compound.

3.2. Tandem mass spectrometric characterization of microcystins

In the absence of suitable standards, information on the retention times, UV absorbances, and molecular masses is not sufficient to confirm the structures of the different microcystins. The application of tandem mass spectrometric techniques to the sequencing of cyclic peptides, such as microcystins, is a well-established analytical technique in many laboratories [57]. Rinehart et al. [21] have developed a protocol using MS and MS–MS for the sequencing and structural assignment of microcystins involving: (1) precise molecular mass measurements using high-resolution FABMS; (2) determination of the amino acids present by NMR and gas chromatography–mass spectrometry (GC–MS); (3) linearization of the peptide by treatment with O_3, $NaBH_4$, and HCl; (4) assignment of the structure of the cyclic and linear peptides using tandem mass spectrometry. They observed fragment ions characteristic of microcystins, which could be used to support structural assignments [12,21].

Alternatively, tandem mass spectra can be obtained for cyanobacterial extracts using combined LC–MS–MS [37]. In the present investigation we have used this approach to confirm the identities of suspected microcystins. In order to assist the assignment of structures of fragment ions observed in the MS–MS spectra of microcystins, the m/z values were compared with those obtained from MS–MS spectra of ^{15}N labelled analogues isolated after stable-isotope feeding experiments. The MS–MS spectra of selected precursor ions of microcystin-LR and of its ^{15}N analogue, obtained from LC–MS–MS analyses of appropriate extracts of *M. aeruginosa* PCC 7820, are presented in Fig. 4a and b, respectively. Under the present experimental conditions, the formation of intense fragment ions from the singly charged $[M + H]^+$ precursor ion required collisional activation with argon at collision energies of at least 50 eV. Valuable

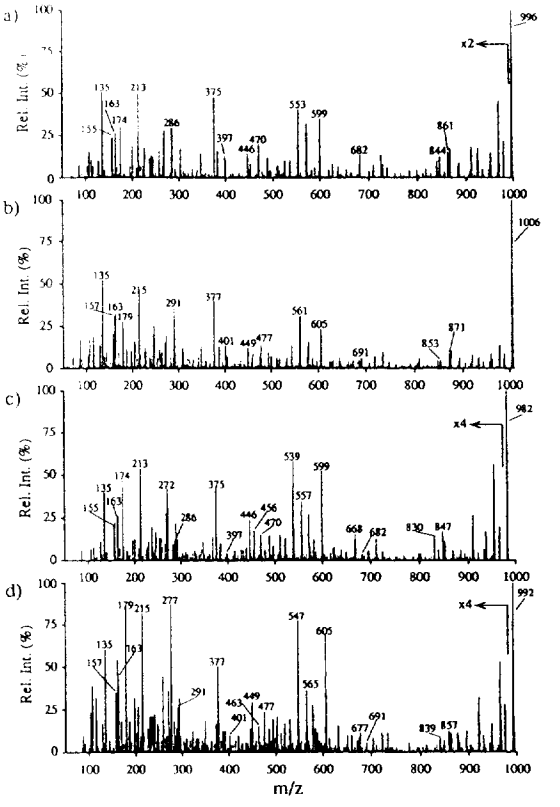

Fig. 4. Extracted product ion spectra from the LC–MS–MS analysis of an extract of *M. aeruginosa* PCC 7820 grown on natural nitrate and culture media fortified with ^{15}N. Product ion of m/z 995.5 from microcystin-LR (a), m/z 1005.5 from ^{15}N microcystin-LR (b), m/z 981.5 from desmethyl microcystin-LR (c), and m/z 991.5 from ^{15}N desmethyl microcystin-LR (d). Conditions: chromatographic conditions as for Fig. 2, collisional activation was achieved using argon target gas at 50 eV collision energy and a collision gas thickness of $3.5 \cdot 10^{15}$ atoms/cm^2.

sequence information could also be deduced from the $[M + 2H]^{2+}$ ion at lower collision energies, although the intensity of this precursor ion was substantially lower than that of the singly protonated molecule.

Fragment ions observed for microcystin-LR arose predominantly from consecutive cleavages of peptide bonds [12,21,57]. Such fragment ions thus provide information concerning different peptide segments of the original molecule, and can be used to verify possible sites of substitution in other microcystins. The sequence information and m/z values obtained from the MS–MS

spectra of microcystin-LR are conveniently summarized in Table 1. Assignment of the fragment ions and their corresponding structures was further confirmed by the mass shift observed for the ^{15}N analogue. The ^{15}N isotopically enriched extract has an $[M+H]^+$ ion at m/z 1005.5 for microcystin-LR, confirming the expected incorporation of ten atoms of ^{15}N. The number of nitrogen atoms for each fragment ion could be deduced from the difference in m/z values observed from the two MS–MS spectra.

The MS–MS spectrum of the desmethyl microcystin-LR (Fig. 4c) and that of its ^{15}N analogue (Fig. 4d) show a similar series of sequence ions, with the exception that the fragment ion at m/z 553 (Fig. 4a) is now shifted to m/z 539, consistent with the proposal that this ion contains one residue lacking a methyl group. Closer examination of Fig. 4c indicated that major fragment ions bearing the Mdha residues at m/z 213 and 375 remained unshifted, indicating that this residue is not the site of desmethylation. However, the fragment ion m/z 286 containing a Masp residue (Fig. 4a) was partly displaced to m/z 272, indicating that in some (not all) of the desmethyl analogues, the Masp residue was replaced by Asp. Interestingly, much less intense fragment ions were also observed at m/z 199, 361, and 286, suggesting that substitution of a methyl group could also take place at the Mdha residue. This proposal was further supported by observations made during CE–ESMS analysis of this extract (see following section).

A characteristic feature of the MS–MS spectra of microcystins is the presence of a set of common fragment ions [15]. As discussed earlier, the variation in the known microcystins is largely due to substitution of two specific amino acids in the cyclic structure (Fig. 1). Fragment ions corresponding to the more conserved por-

Table 1
Assignment of fragment ions observed in product ion spectra of natural and ^{15}N enriched microcystin-LR and desmethyl microcystin-LR

Fragment ions	Microcystin-LR		Desmethyl microcystin-LR	
	^{14}N	^{15}N	^{14}N	^{15}N
$PhCH_2CH(OMe)^+$	135	135	135	135
[Mdha-Ala + H]$^{+a}$	155	157	155	157
$[C_{11}H_{14}O+H]^+$	163	163	163	163
$[Arg+NH_3+H]^+$	174	179	174	179
[Glu-Mdha + H]$^+$	213	215	213	215
[Arg-Masp + H]$^{+b}$	286	291	286	291
[Arg-Asp + H]$^+$	–	–	272	277
$[C_{11}H_{14}O$-Glu-Mdha + H]$^+$	375	377	375	377
[Glu-Mdha-Ala-Leu + H]$^+$	397	401	397	401
$[C_{11}H_{14}O$-Glu-Mdha-Ala + H]	446	449	446	449
[Arg-Asp-Leu-Ala + H]$^+$	–	–	456	463
[Arg-Masp-Leu-Ala + H]$^+$	470	477	470	477
[Arg-Asp-Leu-Ala-Mdha + H]	–	–	539	547
[Arg-Masp-Leu-Ala-Mdha + H]$^+$	553	561	553	561
[Adda-Arg-Masp + H]$^{+c}$	599	605	599	605
[Glu-dha-Ala-Leu-Masp-Arg + H]$^+$	–	–	668	677
[Glu-Mdha-Ala-Leu-Masp-Arg + H]$^+$	682	691	682	691
$[C_{11}H_{14}O$-Glu-Dha-Ala-Leu-Masp-Arg + H]$^+$	–	–	830	839
$[C_{11}H_{14}O$-Glu-Mdha-Ala-Leu-Masp-Arg + H]$^+$	844	853	844	853
Loss of PhCH = CH(OMe)	861	871	847	857

[a] Mdha = N-methyldehydroalanine.
[b] Masp = β-methylaspartic acid.
[c] Adda = 3-amino-9-methoxy-2,6,8-trimethyl-10-phenyldeca-4,6-dienoic acid.

tion of the molecule can thus be used as possible diagnostic ions for the identification of microcystins. These ions include $PhCH_2CH(OMe)^+$ (m/z 135), $[Glu\text{-}Mdha + H]^+$ (m/z 213), and $[C_{11}H_{14}O\text{-}Glu\text{-}Mdha + H]^+$ (m/z 375), see Fig. 4 and Table 1. Suspected microcystins would be expected to give rise to at least one of these ions in the product ion MS–MS spectra of their corresponding $[M + H]^+$ ions. Conversely, it is possible to use one of these three fragment ions in precursor-ion scan mode to identify putative microcystins present in cell extracts. An example of this approach is presented in Fig. 5, obtained by analysis of an extract from *M. aeruginosa* PCC 7820 by direct flow injection. In this case, the third quadrupole Q3 was set to transmit the characteristic microcystin fragment at m/z 135, formed in the RF-only collision cell Q2, while the first quadrupole Q1 was scanned over the range m/z 950–1050. In addition to the expected microcystin-LR at m/z 995.5, other precursor ions of m/z 135 were also observed at m/z 952.5, 972.5, 986.5, 981.5, 1002.5, 1009.5, and 1025.5. Tentative assignments were proposed above for some of these compounds based on data available from both LC–UV and LC–ESMS analyses. The only exceptions to this were the compounds at m/z 972.5, 1009.5, and 1025.5, which could not be matched with any of the known microcystins. In order to confirm the structure of previously assigned microcystins, and to provide further structural information on other related hepatotoxins, additional experiments using combined LC–MS–MS were undertaken.

Examples of product ion spectra for m/z 987.5, 972.2, 1009.5, and 1025.5, obtained from LC–MS–MS analysis of an extract of *M. aeruginosa* PCC 7820, are presented in Fig. 6. The MS–MS spectrum of the microcystin shown in Fig. 6a was consistent with that of microcystin-LF. The observation of characteristic fragment ions at m/z 135, 213, and 375 supported the proposal that this compound was a microcystin. The presence of a phenylalanine residue at position **Z** in the microcystin structure (Fig. 1) was substantiated by the observation of intense fragment ions at m/z 544, 673, and 836. The structures and assignment of some of the fragment ions observed for microcystin-LF are presented in Table 2, together with data extracted from MS–MS spectra of other microcystins analyzed in this study.

Information obtained from the MS–MS spectra of microcystin-LR, -LF, and isomers of

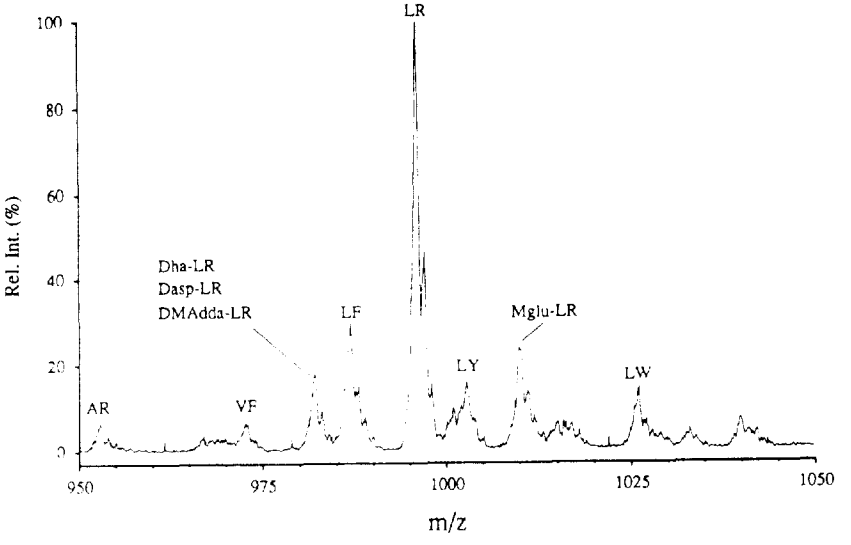

Fig. 5. Precursor ion spectrum of m/z 135 obtained from the direct flow injection of 2 μl of an extract of *M. aeruginosa* PCC 7820. MS–MS conditions as for Fig. 4.

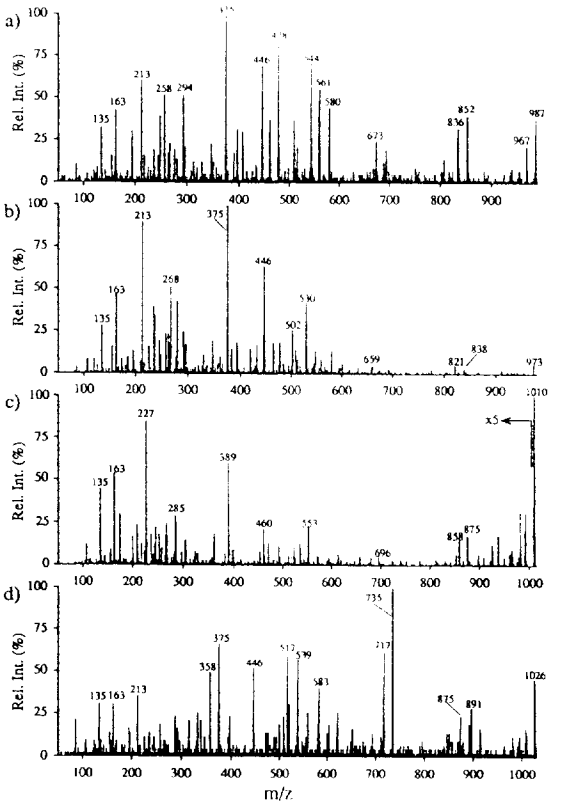

Fig. 6. Extracted MS–MS spectra from the LC–MS–MS analysis of an extract of *M. aeruginosa* PCC 7820. Product ion spectra for *m/z* 987.5 (a), 972.5 (b), 1009.5 (c), and 1025.5 (d). Conditions as for Fig. 4.

desmethyl-LR was used to suggest possible structures for other suspected microcystins. Of particular interest to the present investigation was the observation of three previously unknown microcystins at *m/z* 972.5 (Fig. 6b), 1009.5 (Fig. 6c), and 1025.6 (Fig. 6d). As mentioned in the previous section, the last compound was presumed to be microcystin-LW. This proposal was further supported by the observation of fragment ions at *m/z* 583, 735, and 875 (Table 2, Fig. 6d), which confirmed the presence of a tryptophan residue at position **Z** in Fig. 1. Peptides containing this amino acid give rise to characteristic immonium and indole ions at *m/z* 159 and 130, respectively.

The MS–MS spectrum of the compound with $[M+H]^+$ at *m/z* 1009.5 (Fig. 6c, Table 2) was consistent with a microcystin-LR containing a methylated Glu residue (Mglu). The occurrence of a Glu methyl ester of microcystin-LR has been previously reported in species of *Anabaena flos aquae* CYA 83/1 [58], but not from *M. aeruginosa*. Based on this information alone, it is, however, not possible to ascertain whether the incorporation of the extra methyl group takes place on the carboxylic acid or the α-carbon of Glu or even on the amide nitrogen. Finally, the product ion spectrum of *m/z* 972.5 is presented in Fig. 6b. Fragment ions observed for this compound suggest that the **X** and **Z** position (Fig. 1) are both substituted. The presence of arginine, which is usually characterized by a fragment ion at *m/z* 174, could not be observed for this microcystin. Comparison of this MS–MS spectrum with that of microcystin-LF (Fig. 6a, Table 2) revealed similar fragment ion patterns displaced by 14 Da. More particularly, fragment ions at *m/z* 530, 659, and 822 (Table 2, Fig. 6b) suggests that this microcystin could contain valine and phenylalanine at position **X** and **Z**, respectively (Fig. 1). Further confirmation of this hypothesis will require more elaborate studies involving preparative HPLC, NMR spectroscopy, and amino acid analyses of purified fractions.

3.3. CE–MS and CE–MS–MS analyses of cell extracts

The application of CE–UV to the confirmation of microcystins in fractions collected from preparative HPLC linked with the protein phosphatase assay, was recently demonstrated by Boland et al. [39]. The concentration detection limit was estimated to be approximately 3 μg/ml (30 nl injection) for microcystin-LR analyzed by CE–UV with detection at 200 nm. Separation of microcystins was performed using a Tris buffer with pH 6. However, when coupled to ESMS this buffer can lead to substantial chemical noise and associated loss in sensitivity. Different electrophoretic conditions were therefore developed for the separation of microcystins by CE–ESMS.

Previous investigations using CE–ESMS with acidic buffers and capillaries coated with cationic polymers such as hexadimethrine bromide, have

Table 2
Characteristic fragment ions observed for different microcystins analyzed by LC–MS–MS

Assignment[a]	*m/z* values					
	AR	LF	LY	LW	VF	Mglu-LR
$[M+H]^+$	953	987	1003	1026	973	1010
Loss of PhCH = CH(OMe)	818	852	868	891	838	875
$PhCH_2CH(OMe)^+$	135	135	135	135	135	135
$[C_{11}H_{14}O+H]^+$	163	163	163	163	163	163
[Glu-Mdha + H]$^+$	213	213	213	213	213	227
$[C_{11}H_{14}O$-Glu-Mdha + H]$^+$	375	375	375	375	375	389
$[C_{11}H_{14}O$-Glu-Mdha-Ala + H]$^+$	446	446	446	446	446	460
[**Arg**-Masp-**Ala**-Ala-Mdha + H]$^+$	510	–	–	–	–	–
[**Arg**-Masp-**Ala**-Ala-Mdha-Glu + H]$^+$	639	–	–	–	–	–
[**Arg**-Masp-**Ala**-Ala-Mdha-Glu-$C_{11}H_{14}O$ + H]$^+$	801	–	–	–	–	–
[**Phe**-Masp-**Leu**-Ala-Mdha + H]$^+$	–	544	–	–	–	–
[**Phe**-Masp-**Leu**-Ala-Mdha-Glu + H]$^+$	–	673	–	–	–	–
[**Phe**-Masp-**Leu**-Ala-Mdha-Glu-$C_{11}H_{14}O$ + H]$^+$	–	836	–	–	–	–
[**Tyr**-Masp-**Leu**-Ala-Mdha + H]$^+$	–	–	559	–	–	–
[**Tyr**-Masp-**Leu**-Ala-Mdha-Glu + H]$^+$	–	–	688	–	–	–
[**Tyr**-Masp-**Leu**-Ala-Mdha-Glu-$C_{11}H_{14}O$ + H]$^+$	–	–	852	–	–	–
[**Trp**-Masp-**Leu**-Ala-Mdha + H]$^+$	–	–	–	583	–	–
[CO-Masp-**Leu**-Ala-Mdha-Glu-$C_{11}H_{14}O$ + H]$^+$	–	–	–	735	–	–
[**Trp**-Masp-**Leu**-Ala-Mdha-Glu-$C_{11}H_{14}O$ + H]$^+$	–	–	–	875	–	–
[**Phe**-Masp-**Val**-Ala-Mdha + H]$^+$	–	–	–	–	530	–
[**Phe**-Masp-**Val**-Ala-Mdha-Glu + H]$^+$	–	–	–	–	659	–
[**Phe**-Masp-**Val**-Ala-Mdha-Glu-$C_{11}H_{14}O$ + H]$^+$	–	–	–	–	822	–

[a] The bold amino acids correspond to positions **X** and **Z** in Fig. 1.

enabled identification of a number of peptides, glycopeptides, and proteins in the low femtomole range [53,59]. Such cationic coatings not only reduce the extent of solute–wall interactions but also reverse the direction of the electroosmotic flow (anodal flow), a situation which can magnify the velocity differences amongst those analytes having electrophoretic mobilities in the opposite direction. Furthermore, it is possible to manipulate the electroosmotic flow by varying the acidity of the electrolyte in order to enhance the resolution of analytes having similar electrophoretic mobilities. Preliminary CE–UV experiments, using 50 μm × 107 cm capillaries coated with 5% hexadimethrine bromide and 2% ethylene glycol, indicated that the electroosmotic flow varied from $6.7 \cdot 10^{-8}$ to $4.3 \cdot 10^{-8}$ $m^2 V^{-1} s^{-1}$ for concentrations of formic acid ranging from 0.1 to 2.0 *M*. For the same range of formic acid concentration, the electrophoretic mobility of microcystin-LR was typically $7.4 \cdot 10^{-9}$ $m^2 V^{-1} s^{-1}$ in the opposite direction. Optimized conditions, in terms of both separation efficiencies and analysis time, were achieved using 1.0 *M* formic acid, and yielded plate counts in the order of 800 000 for microcystin-LR standards based on measurements of peak width at half height. Such electrophoretic conditions were also found to be compatible with the operation of electrospray ionization.

The CE–ESMS analysis of a 10 μg/ml standard of microcystin-LR is shown in Fig. 7. Under the specified conditions, microcystin-LR is observed as a sharp peak migrating at 8.95 min in Fig. 7b. Two peaks corresponding to desmethyl microcystin-LR were also observed, at 8.98 and 9.09 min in the extracted ion chromatogram obtained from the same analysis (Fig. 7a). The fact that this toxin standard contains sizable amounts of the desmethyl analogue probably reflects the difficulty in separating these closely related compounds by chromatographic meth-

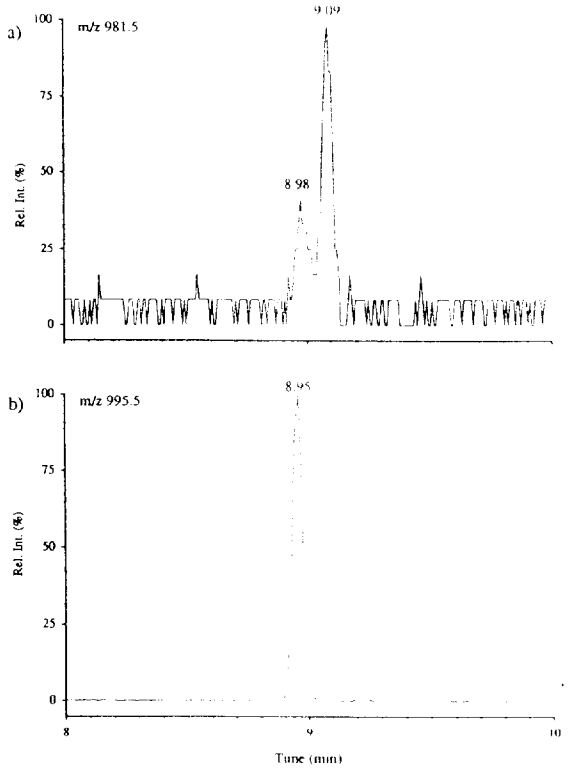

Fig. 7. CE–ESMS analysis of 10 μg/ml microcystin-LR standard using SIM for *m/z* 981.6 (a) and 995.6 (b). Conditions: fused-silica column 1.0 m × 50 μm I.D. coated with 5% Polybrene, 2% ethylene glycol, 20 nl injection, 1.0 *M* formic acid electrolyte, sheath liquid: 25% aqueous methanol (0.2% formic acid) at a flow-rate of 7 μl/min.

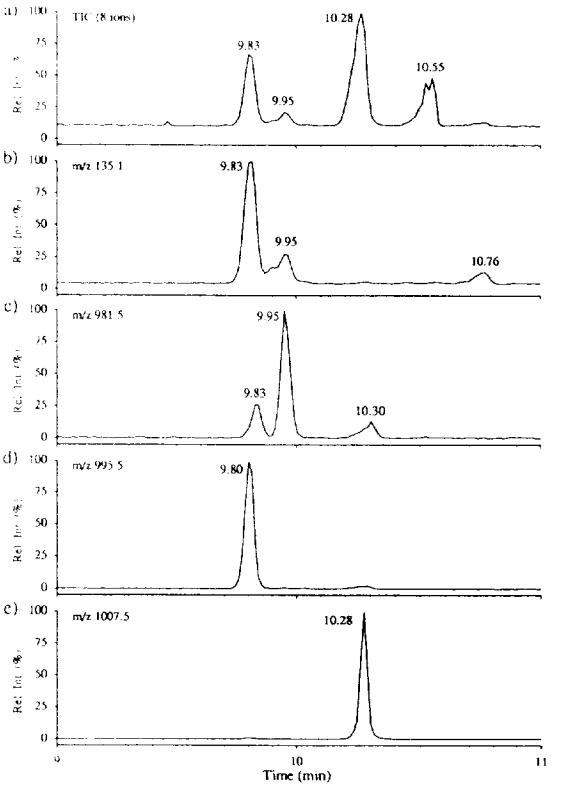

Fig. 8. CE–ESMS analysis of a methanol extract from *M. aeruginosa* UTEX LB 2385 using SIM for the sum of ion current for *m/z* 121.1, 135.1, 692.5, 981.5, 995.5, 1007.5, 1027.5, 1041.5 (a). Extracted ion chromatograms for 135.1 (b), 981.5 (c), 995.5 (d), 1007.5 (e). Conditions as for Fig. 7, except that a voltage of 100 V was applied at the orifice.

ods. Purification of microcystin-LR from cell extracts using reversed-phase HPLC is thus likely to result in a product containing trace amounts of desmethyl microcystin-LR, and qualitative analysis with complementary separation techniques such as CE must be done to evaluate purity of commercially available standards.

CE–ESMS analysis (using selected ion monitoring) of a cyanobacterial extract obtained from *M. aeruginosa* UTEX LB 2385 is shown in Fig. 8. The reconstruction ion electropherogram corresponding to the sum of intensities of *m/z* 121.1, 135.1, 692.5, 981.5, 995.5, 1007.5, 1027.5, and 1041.5, is shown in Fig. 8a. In order to facilitate identification of potential hepatotoxins present in complex extracts, mass spectral ionization conditions were selected to promote the formation of characteristic fragment ions common to most microcystins. Fragmentation reactions leading to a loss of 134, or conversely the formation of *m/z* 135 from the Adda residue, were found to be a common feature in the mass spectra of the microcystins (Fig. 4). The formation of these fragment ions was promoted by increasing the voltage of the skimmer/orifice lens to 100 V. The extracted ion chromatogram for *m/z* 135 is shown in Fig. 8b, and reveals the presence of at least four putative microcystins.

The extracted ion electropherograms for *m/z* 981.5 and 995.5 are shown in Figs. 8c and 8d, respectively. Interestingly, the electropherogram for *m/z* 981.5 (Fig. 8c) shows three resolved peaks migrating at 9.8, 9.9, and 10.2 min. As will

be discussed later, these peaks were found to be closely related isomers differing only in the position of a methyl group (Fig. 1). Peaks identified in the m/z 135 trace under these conditions matched those of microcystin-LR and its desmethyl analogues. Only the desmethyl microcystin-LR with the lowest abundance does not show a peak in the m/z 135 electropherogram. As will be mentioned later, this compound was found to contain a modified desmethyl Adda residue, and thus could not form the characteristic m/z 135 fragment ion. The small peak observed in the extracted ion chromatogram of m/z 995.5 (Fig. 8d) at 10.3 min is possibly due to a geometrical isomer of microcystin-LR. Previous investigations have shown the presence of a (**Z**) Adda isomer of microcystin-LR in extracts of *M. viridis* [60]. It is noteworthy that this additional peak was not observed in the LR standard analyzed under the same conditions (Fig. 7b).

In several cases, compounds devoid of the Adda residue did not give rise to a fragment ion at m/z 135. Such discrimination is illustrated in Fig. 8e for an unknown component with $[M+H]^+$ at m/z 1007.5, present in the *M. aeruginosa* UTEX LB extract, and for which no significant signal was observed in the m/z 135 trace. The formation of a m/z 135 fragment ion can be used as a screening method for monitoring microcystins in cell extracts. However, one must be aware that microcystins present at low concentrations (<20 pg) may not be detected in this way, and although the majority of microcystins produce the m/z 135 ion, this might not be a valid generalization for all related hepatotoxins.

In order to identify individual isomers of desmethyl microcystin-LR, further experiments using CE in combination with tandem mass spectrometry were undertaken. Previous analyses of cyanobacterial extracts have identified three desmethylated microcystins, differing only in the site of demethylation (Fig. 1) [12,36,41,46,47]. Because of sensitivity considerations, CE–MS–MS analyses were achieved using multiple reaction monitoring mode (MRM). As mentioned earlier, microcystins produce characteristic fragment ions which can be used to confirm the amino acid sequence assignments (Figs. 4 and 6, Tables 1 and 2). Proper selection of reaction channels enabled identification of each desmethyl microcystin-LR isomer identified in Fig. 8c. The observation of fragment ions differing by 14 Da from those of microcystin-LR suggested possible sites of substitution. For example, substitution of the Adda residue by a desmethyl homologue will give rise to a fragment ion at m/z 121 instead of m/z 135. Similarly, substitution on the Masp residue will be indicated by a $[\text{Arg-Asp}+H]^+$ fragment ion at m/z 272 instead of m/z 286, whereas a demethylation of the Mdha residue will be reflected by the observation of a fragment ion at m/z 361, corresponding to $[C_{11}H_{14}O\text{-Glu-Dha}+H]^+$.

The analysis of the same methanol extract as

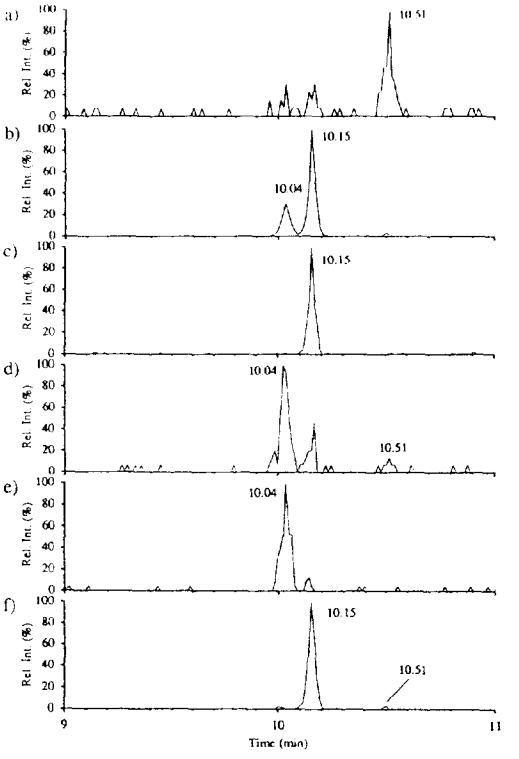

Fig. 9. CE–MS–MS analysis of a methanol extract from *M. aeruginosa* UTEX LB 2385 using multiple reaction monitoring for transitions 981.6→121.1 (a), 981.6→135.1 (b), 981.6→272.3 (c), 981.6→286.3 (d), 981.6→361.3 (e), and 981.6→375.3 (f). Electrophoretic and MS–MS conditions as for Fig. 7 and 4, respectively.

used in Fig. 8 is presented in Fig. 9 for the dissociation of the precursor ion m/z 981.6 using CE–MS–MS in MRM mode. The transitions monitored for the Adda residue (Figs. 9a and 9b) show one peak at 10.5 min for the desmethylated isomer (m/z 121) and two peaks at 10.0 and 10.2 min for the two isomers containing the Adda residue (m/z 135). The second component migrating at 10.2 min was found to contain an Asp residue, based on the ion profile obtained for transitions leading to the formation of m/z 272 (Fig. 9c). The desmethyl microcystins-LR containing a Masp residue were observed at 10.0 and 10.5 min in Fig. 9d. It is noteworthy that because of the high abundance of the second component, the peak observed at 10.2 min in Fig. 9d is probably due to the [Glu-Mdha-Ala + H]$^+$ fragment ion at m/z 285. The final two transitions used in the MRM experiments (Figs. 9e and 9f) enabled identification of Dha-microcystin-LR. The transition 982→361 showed one peak at 10.0 min for the expected [$C_{11}H_{14}O$-Glu-dha + H]$^+$ fragment ion, whereas Fig. 9f shows a prominent signal at 10.2 min accompanied by a weaker peak at 10.5 min for the two remaining microcystins, bearing the Mdha residue.

3.4. Quantitation of microcystin-LR by LC–ESMS and CE–ESMS

The amount of microcystin-LR present in extracts of *M. aeruginosa* cells was determined using both LC–ESMS and CE–ESMS operating in SIM mode. The dependence of peak area on sample concentration was examined for a fixed injection volume of microcystin-LR (10 μl for LC and 20 nl for CE). Fig. 10 shows typical calibration curves for these two techniques. In both cases, good linearity with correlation coefficient $r^2 > 0.9990$ was found over concentrations ranging from two to three orders of magnitude. The insets in Fig. 10 correspond to traces obtained for concentrations approaching the detection limits. The LC–ESMS chromatogram corresponding to the on-column injection of 500 pg (0.05 μg/ml) of microcystin-LR, using SIM, for m/z 995.5 gave a signal to noise (S/N) ratio of

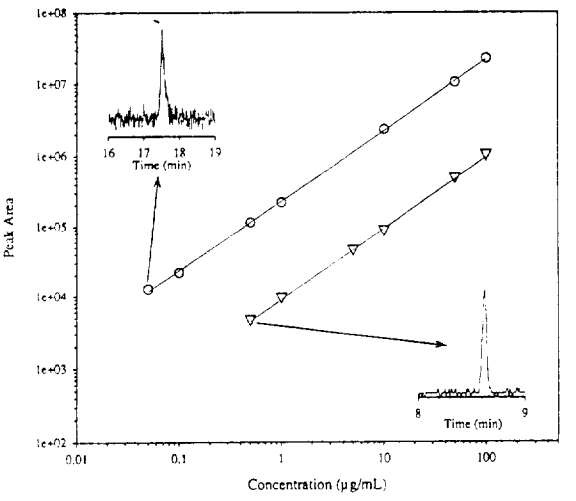

Fig. 10. Calibration plots of concentration versus peak areas for the analysis of microcystin-LR using LC–ESMS (circles), $r^2 = 0.9992$, and CE–ESMS (triangles), $r^2 = 0.9994$. Insets show the peak profiles at the lowest concentration analyzed by both techniques.

approximately 5:1. In fact, the actual amount of microcystin-LR introduced to the mass spectrometer was approximately 50 pg (50 fmol), taking into account that a post-column split of 1:10 was used.

In comparison, the electropherogram obtained for a 20 nl injection of a 0.5 μg/ml solution of microcystin-LR gave a S/N ratio of approximately 10:1. In this case, the detection limit for CE–ESMS was estimated as 0.2 μg/ml for an actual injection of 4 pg (4 fmol) of microcystin-LR. Despite the lower injection sizes typically used in zone electrophoresis format, the concentration detection limit observed for CE–ESMS was found to be higher than that of LC–ESMS by less than an order of magnitude. On the other hand, the mass detection limit observed for CE–ESMS was found to be higher by at least an order of magnitude compared to that of LC–ESMS. The enhanced signal strength observed here is attributed to the higher separation efficiencies obtainable with CE–ESMS. For typical 20 nl injection (17% of the capillary volume), plate counts obtained for microcystin-LR were approximately 230 000 over the concentration range examined.

Such high separation efficiencies imposed considerable demands on the mass spectrometer for analyses requiring broader acquisition mass ranges. CE–ESMS analysis conducted under full mass scan acquisition (m/z 400–1200) required a concentration of 5 μg/ml of microcystin-LR in order to obtain a meaningful mass spectrum, whereas similar-quality information could be obtained for solutions ten times less concentrated using LC–ESMS. The relatively high concentration detection limit of CE has been one of the limitations of the present method. However, recent experiments performed in this laboratory using capillary isotachophoresis pre-concentration have shown promising results for enhancing the concentration detection limit of microcystin-LR analyzed subsequently using zone electrophoresis. Results from these studies will be presented separately.

The concentration of microcystin-LR present in the two strains of *M. aeruginosa* investigated was determined using both LC–ESMS and CE–ESMS. For similar weights of biomass extracted, higher concentrations of microcystin-LR were consistently found in extracts of cells from the UTEX LB 2385 strain. Quantitative analyses ($n = 3$) of extracts of this strain, performed using SIM acquisition mode, showed concentrations of microcystin-LR of 11.8 ± 0.9 μg/ml (using CE–ESMS), and 8.0 ± 0.3 μg/ml (using LC–ESMS). When converted in terms of weight equivalent of cells extracted, these concentrations represent 110–150 μg of microcystin-LR per gram of wet cyanobacterial cells. In contrast, the corresponding amounts of microcystin-LR in extracts of cells from PCC 7820 were 4.3 ± 0.5 μg/ml using CE–ESMS and 2.8 ± 0.1 μg/ml for LC–ESMS. Such concentrations actually represent 6–10 μg per gram of wet cyanobacterial cells. As observed, concentrations determined using CE–ESMS were consistently 25% higher than those obtained using LC–ESMS. These results were considered to be in acceptable agreement with each other, considering that these analyses were performed on different occasions, one month apart. The higher relative standard deviations observed for concentrations obtained with CE–ESMS were associated with the use of unsealed vials, thus allowing more extensive evaporation of the sample solvent. Minimization of sample handling errors, evaporation of solvent, and other associated sources of uncertainties, can be minimized using suitable internal standards spiked in the original cell extract.

4. Conclusions

Microcystins present at low μg/ml levels in cell extracts of *M. aeruginosa* were analyzed directly by LC–ESMS and CE–ESMS. Analyses performed in selected ion monitoring mode provided detection limits (S/N 3:1) in the order of 50 nM for microcystin-LR using LC–ESMS and 200 nM for analyses conducted with CE–ESMS. Mass spectral detection provided enhanced selectivity compared to UV detection, and meaningful spectra were generally obtained for microcystins present at levels as low as 500 nM in extracts of *M. aeruginosa* cells using LC–ESMS. One distinct advantage of CE–ESMS over LC–ESMS was the possibility of separating isomers differing only in the position of a single methyl group on the microcystin backbone structure. CE–ESMS analyses obtained using capillaries dynamically coated with hexadimethrine bromide and ethylene glycol enabled identification of three desmethyl isomers of microcystin-LR, differing in the Adda, Masp, or Mdha residue. Further characterization of these positional isomers was performed using CE in combination with tandem mass spectrometry.

Selective identification of microcystins present in extracts of toxic cyanobacterial cells was facilitated using a precursor-ion scan of m/z 135, a fragment ion characteristic of the Adda residue. Suspected microcystins were subsequently analyzed using LC–MS–MS to obtain amino acid sequence information, and to identify possible sites of amino acid substitution. Rationalization of fragment ions observed in the MS–MS spectra of microcystins was possible using methanolic extracts of cell cultures of *M. aeruginosa* grown on natural and ^{15}N-labelled nitrate nutrients. More importantly, the present investigation has emphasized the potential of CE and LC in

combination with tandem mass spectrometry for the identification of known and potentially novel microcystins. In particular, this study has shown evidence for two previously unknown hepatotoxins, microcystin-LW and microcystin-VF, in extracts of *M. aeruginosa* PCC 7820.

Acknowledgements

The authors would like to thank Dr. Judy Needham for providing methanol extracts of *M. aeruginosa* cells used in the preliminary development stages of this study. The technical assistance of Melanie Hoare in preparing cell cultures is also gratefully acknowledged. K.P.B. would like to acknowledge funding from the Walter C. Summer Fellowship.

References

[1] G.A. Codd and G.K. Poon, in L.J. Rogers and J.G. Gallon (Editors), Biochemistry of the Algae and Cyanobacteria, Clarendon Press, Oxford, 1988, p. 283.
[2] W.W. Carmichael, in A.T. Tu (Editor), Handbook of Natural Toxins, Marcel Dekker, New York, 1988, p.121.
[3] J.A.O. Meriluoto, S.E. Nygård, A.M. Dahlem and J.E. Eriksson, Toxicon, 28 (1990) 1439.
[4] H.W. Siegelman, W.H. Adams, R.D. Stoner and D.N. Slatkin, in E.P. Ragelis (Editor), Seafood Toxins, American Chemical Society, Washington, DC, 1984, p. 407.
[5] M.T.C. Runnegar, R.G. Gerdes and I.R. Falconer, Toxicon, 29 (1991) 43.
[6] W.C. Theiss, W.W. Carmichael, J. Wyman and R. Bruner, Toxicon, 26 (1988) 603.
[7] M.T.C. Runnegar, J. Andrews, R.G. Gerdes and I.R. Falconer, Toxicon, 25 (1987) 1235.
[8] J.E. Eriksson, G.I.L. Paatero, J.A.O. Meriluoto, G.A. Codd, G.E.N. Kass, P. Nicotera and S. Orrenius, Exp. Cell Res., 185 (1989) 86.
[9] A.S. Dabholkar and W.W. Carmichael, Toxicon, 25 (1987) 285.
[10] M.T.C. Runnegar and I.R. Falconer, Toxicon, 24 (1986) 109.
[11] W.W. Carmichael, J.W. He, Z.R. He and Y.M. Juan, Toxicon, 26 (1988) 1213.
[12] M. Namikoshi, K.L. Rinehart, R. Sakai, R.R. Stotts, A.M. Dahlem, V.R. Beasley, W.W. Carmichael and W.R. Evans, J. Org. Chem., 57 (1992) 866.
[13] A. Kungsuwan, T. Noguchi, S. Matsunaga, M.F. Watanabe, S. Watabe and K. Hashimoto, Toxicon, 26 (1988) 119.
[14] J.A.O. Meriluoto, A. Sandström, J.E. Eriksson, G. Remaud, A.G. Craig and J. Chattopadhyaya, Toxicon, 27 (1989) 1021.
[15] D.M. Toivola, J.E. Eriksson and D.L. Brautigan, FEBS Lett., 344 (1994) 175.
[16] R.E. Honkanen, J. Zwiller, R.E. Moore, S. Daily, B.S. Khatra, M. Dukelow and A.L. Boynton, J. Biol. Chem., 265 (1990) 19401.
[17] C. MacKintosh, K.A. Beattie, S. Klumpp, P. Cohen and G.A. Codd, FEBS Lett., 264 (1990) 187.
[18] R. Nishiwaki-Matsushima, S. Nishiwaki, T. Ohta, S. Yoshiawa, M. Suganuma, K.-I. Harada, M.F. Watanabe and H. Fujiki, Jpn. J. Cancer Res., 82 (1991) 993.
[19] R. Nishiwaki-Matsushima, T. Ohta, S. Nishiwaki, M. Suganuma, K. Kohyama, T. Ishikawa, W.W. Carmichael and H. Fujiki, J. Cancer Res. Clin. Oncol., 118 (1992) 420.
[20] W.W. Carmichael, Sci. Am., January (1994) 78.
[21] K.L. Rinehart, M. Namikoshi and B.W. Choi, J. Appl. Phycol., 6 (1994) 159.
[22] W.W. Carmichael, J. Appl. Bacteriol., 72 (1992) 445.
[23] D.P. Botes, C.C. Viljoen, H. Kruger, P.L. Wessels and D.H. Williams, S. Afr. J. Sci., 78 (1982) 378.
[24] D.P. Botes, A.A. Tuinman, P.L. Wessels, C.C. Viljoen, H. Kruger, D.H. Williams, S. Santikarn, R.J. Smith and S.J. Hammond, J. Chem. Soc. Perkin Trans. 1, (1984) 2311.
[25] D.P. Botes, C.C. Viljoen, H. Kruger, P.L. Wessels and D.H. Williams, Toxicon, 20 (1982) 1037.
[26] K.L. Rinehart, K.-I. Harada, M. Namikoshi, C. Chen and C.A. Harvis, J. Am. Chem. Soc., 110 (1988) 8557.
[27] W.W. Carmichael, V. Beasley, D.L. Bunner, J.N. Eloff, I. Falconer, P. Gorham, K.-I. Harada, T. Krishnamurthy, M. Yu, R.E. Moore, K.L. Rinehart, M. Runnegar, O.M. Skulberg and M. Watanabe, Toxicon, 26 (1988) 971.
[28] A.T.R. Sim and L. Mudge, Toxicon, 31 (1993) 1179.
[29] T.W. Lambert, M.P. Boland, C.F.B. Holmes and S.E. Hrudey, Environ. Sci. Technol., 28 (1994) 753.
[30] W.W. Carmichael and P.E. Bent, Appl. Environ. Microbiol., 41 (1981) 1383.
[31] L.A. Lawton, D.L. Campbell, K.A. Beattie and G.A. Codd, Lett. Appl. Microbiol., 11 (1990) 205.
[32] F.S. Chu, X. Huang and R.D. Wei, J. Assoc. Off. Anal. Chem., 73 (1990) 451.
[33] P.S. Gathercole and P.G. Thiel, J. Chromatogr., 408 (1987) 435.
[34] J.A.O. Meriluoto, J.E. Eriksson, K.-I. Harada, A.M. Dahlem, K. Sivonen and W.W. Carmichael, J. Chromatogr., 509 (1990) 390.
[35] K.-I. Harada, M. Suzuki, A.M. Dahlem, V.R. Beasley, W.W. Carmichael and K.L. Rinehart, Toxicon, 26 (1988) 433.
[36] R. Luukkainen, K. Sivonen, M. Namikoshi, M. Färdig,

K.L. Rinehart and S.I. Niemela, Appl. Environ. Microbiol., 59 (1993) 2204.
[37] C. Edwards, L.A. Lawton, K.A. Beattie, G.A. Codd, S. Pleasance and G.J. Dear, Rapid Commun. Mass Spectrom., 7 (1993) 714.
[38] C.F.B. Holmes, Toxicon, 29 (1991) 469.
[39] M.P. Boland, M.A. Smillie, D.Z.X. Chen and C.F.B. Holmes, Toxicon, 31 (1993) 1393.
[40] D.Z.X. Chen, M.P. Boland, M.A. Smillie, H. Klix, C. Ptak, R.J. Andersen and C.F.B. Holmes, Toxicon, 31 (1993) 1407.
[41] T. Krishnamurthy, L. Szafraniec, D.F. Hunt, J. Shabanowitz, J.R. Yates, C.R. Hauer, W.W. Carmichael, O. Skulberg, G.A. Codd and S. Missler, Proc. Natl. Acad. Sci. USA, 86 (1989) 770.
[42] D.P. Botes, P.L. Wessels, H. Kruger, M.T.C. Runnegar, S. Santikarn, R.J. Smith, J.C.J. Barna and D.H. Williams, J. Chem. Soc. Perkin Trans. 1, (1985) 2747
[43] I.M. Birk, U. Matern, I. Kaiser, C. Martin and J. Weckesser, J. Chromatogr., 449 (1988) 423.
[44] I.M. Birk, R. Dierstein, I. Kaiser, U. Matern, W.A. König, R. Krebber and J. Weckesser, Arch. Microbiol., 151 (1989) 411.
[45] K. Sivonen, W.W. Carmichael, M. Namikoshi, K.I. Rinehart, A.M. Dahlem and S.I. Niemela, Appl. Environ. Microbiol., 56 (1990) 2650.
[46] K.-I. Harada, K. Matsuura, M. Suzuki, M.F. Watanabe, S. Oishi, A.M. Dahlem, V.R. Beasley and W.W. Carmichael, Toxicon, 28 (1990) 55.
[47] K. Sivonen, M. Namikoshi, W.R. Evans, M. Färdig, W.W. Carmichael and K.L. Rinehart, Chem. Res. Toxicol., 5 (1992) 464.
[48] F. Kondo, Y. Ikai, H. Oka, N. Ishikawa, M.F. Watanabe, M. Watanabe, K.-I. Harada and M. Suzuki, Toxicon, 30 (1992) 227.
[49] G.K. Poon, L.J. Griggs, C. Edwards, K.A. Beattie and G.A. Codd, J. Chromatogr., 628 (1993) 215.
[50] M. Namikoshi, K.L. Rinehart, A.M. Dahlem and V.R. Beasley, Tetrahedron Lett., 30 (1989) 4349.
[51] S. Pleasance, P. Thibault and J. Kelly, J. Chromatogr., 591 (1992) 325.
[52] S.J. Locke and P. Thibault, Anal. Chem., 66 (1994) 3436.
[53] S. Pleasance and P. Thibault, in P. Camillieri (Editor), Capillary Electrophoresis, Theory and Practice, CRC Press, Boca Raton, FL, 1993, p. 311.
[54] R.D. Smith, J.A. Olivares, N. Nguyen and H.R. Udseth, Anal. Chem., 60 (1988) 436.
[55] R.D. Stoner, W.H. Adams, D.N. Slatkin and H.W. Siegelman, Toxicon, 27 (1989) 825.
[56] S.M.F.O. Azevedo, W.R. Evans, W.W. Carmichael and M. Namikoshi, J. Appl. Phycol., 6 (1994) 261.
[57] K. Eckart, Mass Spectrom. Rev., 13 (1994) 23.
[58] K. Sivonen, O.M. Skulberg, M. Namikoshi, W.R. Evans, W.W. Carmichael and K.L. Rinehart, Toxicon, 30 (1992) 1465.
[59] J.F. Kelly, S.J. Locke, L. Ramaley and P. Thibault, J. Chromatogr. A, in press.
[60] K.I. Harada, K. Ogawa, K. Matsuura, H. Murata, M. Suzuki, M.F. Watanabe, Y. Itezono and N. Nakayama, Chem. Res. Toxicol., 3 (1990) 473.